Tris(indenyl)lanthanoid(III) Sulfoxide Adducts (1:1) in the Solid State and in Solution: Ligand Chirality as a Powerful Diagnostic Tool for Rapid Intermolecular Sulfoxide Exchange and Indenyl $\eta^5 \rightleftharpoons \eta^1$ Fluxionality

Jingwen Guan, Jens Stehr, and R. Dieter Fischer*[a]

Dedicated to Professor Ernst Otto Fischer on the occasion of his 80th birthday

Abstract: Numerous members of the new class of 1:1 adducts: $[LnCp_3 \cdot OSR^1R^2]$ ($Cp = C_5H_5$ or C_9H_7; $R^1/R^2 =$ Me/4-MeC_6H_4 (MTSO) or Ph/Ph (DPSO); Ln = La, Pr, Nd, or Sm) have been prepared and characterized. While solid $[Ln(C_9H_7)_3 \cdot MTSO]$ (C_9H_7 = indenyl; Ln = La, Pr) contains exclusively oxygen-bonded sulphoxide and three η^5-coordinated indenyl ligands in a chiral arrangement around the metal ion, the C_9H_7 ligands of the dissolved paramagnetic molecules (Ln = Pr, Nd, Sm) are involved in rapid $\eta^5 \rightleftharpoons \eta^1$ fluxionality. Both variable-temperature ^{1}H NMR and f–f circular dichroism (CD) spectroscopy indicate that a second chirogenic centre is generated that lies closer to the metal ion than the chiral sulphur atom of the MTSO ligand. In strict contrast, the congeners with $Cp = C_5H_5$ (Ln = Pr, Nd, Yb) are practically CD-silent, although again the Ln–O distances are shorter by about 10 pm than in the corresponding THF adducts. Surprisingly, the NMR spectra of solutions of mixtures of $[Ln(C_9H_7)_3 \cdot MTSO]$ complexes with (*R*)-(+)- *and* (*S*)-(−)-MTSO, or/and with two different metals reveal rapid *inter*-molecular sulphoxide exchange. On the other hand, mutual MTSO/THF exchange seems to be inhibited, which suggests that the facile sulphoxide exchange follows a special mechanistic pathway.

Keywords: circular dichroism · fluxionality · lanthanides · NMR spectroscopy · structure elucidation

Introduction

Although pentahapto (η^5) coordination represents the most common bonding mode of the cyclopentadienyl (Cp) ligand, numerous cases of lower Cp hapticities are known. Often quite puzzling, and almost contradictory features, may accompany the studies of variable-hapticity systems. One classical example is the complex $[Ti(\eta^5\text{-}Cp)_2(\eta^1\text{-}Cp)_2]$, the high-temperature solution NMR spectra of which are, nevertheless, consistent with four virtually equal Cp ligands,[1] whereas the more recently investigated complex $[Sm(\eta^5\text{-}Cp^*)_3]$ ($Cp^* = C_5Me_5$)[2] displays a solution chemistry that could be rationalized in terms of at least short-lived molecules of the type $[Sm(\eta^5\text{-}Cp^*)_2(\eta^1\text{-}Cp^*)]$.[3] Similarly, a lower hapticity than five was repeatedly proposed for the indenyl ligands of the adduct $[Sm(indenyl)_3 \cdot THF]$ (indenyl = C_9H_7) even at room temperature,[4] but was finally ruled out by X-ray crystallography and solution NMR spectroscopy.[5] Currently, we are focusing our interest, in view of the rapidly increasing structural diversity of tris(indenyl)lanthanoid(III) complexes with[5] (and without[6]) one Lewis base molecule, on the new 1:1 adducts with achiral diphenylsulphoxide (DPSO) and chiral methyl-*p*-tolyl-sulphoxide (MTSO). We wish to demonstrate that the use of *both* (*R*)-(+)- and (*S*)-(−)-MTSO provides valuable insights into new details of the structure and reactivity of $[Ln(C_9H_7)_3 \cdot OSRR']$ systems. Interestingly, rapid $\eta^5 \rightleftharpoons \eta^1$ *inter*conversion of indenyl ligands is deduced here from both variable-temperature (VT) NMR and f–f circular dichroism (CD) experiments.

[a] Prof. Dr. R. D. Fischer, Dr. J.-W. Guan,[+] Dr. J. Stehr
Institut für Anorganische und Angewandte Chemie
der Universität Hamburg
Martin-Luther-King-Platz 6, D-20146 Hamburg (Germany)
Fax: (+49) 40-4123-2838
E-mail: fischer@chemie.uni-hamburg.de

[+] Present address: Department of Chemistry, University of Ottawa, Ottawa, Ontario (Canada)

Results and Discussion

Synthesis and general properties of adducts of the general type $[LnCp_3 \cdot OSRR']$: Organometallic sulphoxide complexes of the general composition $[LnCp_3 \cdot OSR^1R^2]$ (Ln = lanthanoid element, $Cp = C_5H_5$ or C_9H_7, R = alkyl or aryl group) have rarely been described in the open literature. Apart from the presentation of the complex $[La(C_5H_5)_3 \cdot OSMe_2]$ as an outstanding candidate for ^{139}La NMR spectroscopy,[7a] only the crystal structures of this compound[7b] and three related $Ln(C_5H_5)_3$ derivatives[9] (see Table 1) have so far been

0947-6539/99/0507-1992 $ 17.50+.50/0 *Chem. Eur. J.* **1999**, *5*, No. 7

Table 1. List of known $[LnCp_3 \cdot OSR^1R^2]$ complexes. Compounds designated by an asterisk have been investigated by X-ray crystallography; **a**: with (*R*)-(+)-MTSO; **b**: with (*S*)-(−)-MTSO.[a]

	Cp = C_9H_7			Cp = C_5H_5		Color
	MTSO		DPSO	MTSO	DPSO	C_9H_7/C_5H_5
La	**1a***[10]	**1b***[11]	**5**[10]	**8a***[15]	**13***[18]	colorless
Pr	**2a***[12]	**2b***[13]	**6**	**9a***[16]	**14***[19]	leek green/yellowish green
Nd	**3a**	**3b**	**7***[14]	**10a***[17]	**15**	green/violet-blue
Sm	**4a**	**4b**	–	**11a**[9]	–	deep red/pale yellow
Yb	–	–	–	**12a***[9]	–	deep green

[a] Moreover, the chiral complex $[Pr(C_5H_5)_3 \cdot (R)$-(+)-OS(2-pyridyl)(*p*-tolyl)] has been characterised both by X-ray crystallography and solution ^{1}H NMR spectroscopy.[9a] The complex $[La(C_5H_5)_3 \cdot DMSO]$[7] has been mentioned in the text.

documented in slightly remote contexts. Detailed spectroscopic properties of the first tris(indenyl) congener (with Pr and (*R*)-(+)-MTSO) have been described,[9a] and we have published more recently the crystal structure of its La homologue **1a** and, inter alia, the ^{1}H NMR spectrum of the first corresponding diphenylsulphoxide (DPSO) adduct **5**.[10] In Table 1, all known adducts with MTSO and DPSO are listed. This table also presents the complete numbering scheme of all sulphoxide complexes referred to here.

All 1:1 sulphoxide adducts can be readily prepared by allowing a suspension of either the corresponding THF adduct or base-free $[LnCp_3]$ in toluene to react with the sulphoxide in a strict 1:1 ratio; removal of excess sulphoxide at a later stage is practically impossible. Usually, the sulphoxide adducts are obtained in excellent yields as polycrystalline precipitates. Owing to considerably better solubilities at elevated temperature, analytically pure and well-crystallized products can be obtained by redissolving the primary product in toluene heated up almost to boiling point, and slow cooling to about 0 °C afterwards. Interestingly, the complexes **3** and **4** (Ln = Nd and Sm) are more soluble in toluene and have so far not afforded single crystals of X-ray quality. While the melting points of all cyclopentadienyl complexes (i.e., **8a**–**10a** and **13**–**15**) lie between 226 and 238 °C, those of the indenyl complexes with MTSO (**1a**–**4b**) are notably lower (128–150 °C) than the melting points of the corresponding DPSO adducts **5**–**7** (180–200 °C).

All indenyl complexes are more sensitive, both thermally and towards traces of air and halogenated solvents, than the corresponding cyclopentadienyl complexes. For instance, while their solubility in dichloromethane exceeds that in toluene, solutions in CH_2Cl_2 tend to age within a few hours. Moreover, even the surfaces of crystals of **2**–**4** kept under pure N_2 darken spontaneously. A substantial red-shift of the $\tilde{\nu}$(SO) bands of the tris(cyclopentadienyl) complexes (Table 2) suggests considerable Ln–O interaction, while in the infrared spectra of the tris(indenyl) complexes the corresponding $\tilde{\nu}$(SO) bands cannot be reliably identified.

Table 2. Red-shift $\Delta\tilde{\nu}$(SO) [cm^{-1}] and Ln–O distances [pm] in $[LnCp_3 \cdot L]$ systems (L = MTSO, DPSO or THF); $\tilde{\nu}$(SO) of MTSO: 1048 cm^{-1}; of DPSO: 1037 cm^{-1}.

	Cp = C_5H_5				Cp = C_9H_7	
	MTSO		DPSO		MTSO/DPSO	THF[4]
	$\Delta\tilde{\nu}$(SO)	*d*(Ln–O)	$\Delta\tilde{\nu}$(SO)	*d*(Ln–O)	*d*(Ln–O)	
La	42	244.4(5)	20	244.3(4)	245.3(5)[a][10]	258.8(9)
					244.1(7)[b]	257.5(2)
Pr	40	241.8(4)	25	244.4(4)	244.2(8)[a]	255.7(7)
					243.2(5)[b]	–
Nd	39	239.0(6)	40	–	238.3(4)[c]	258(2)
				–		251.2(7)
Sm	23	–	–	–	–	–
Yb	21	229.0(7)[9]				239(2)[d]

[a] With (*R*)-(+)-MTSO. [b] With (*S*)-(−)-MTSO. [c] With DPSO. [d] Of $[Lu(C_5H_5)_3 \cdot THF]$.[8]

Solid-state structures from crystallographic studies: Single crystals for X-ray crystallography were grown by slow cooling of warm, concentrated toluene solutions. Suitable solutions of **1** and **2** were best achieved by the addition of small portions of THF. In Figure 1, the molecular structures of two representative examples of the MTSO and DPSO adducts that contain cyclopentadienyl ligands are compared. As expected for the strongly oxophilic Ln^{3+} ions, the sulphoxide molecule is coordinated exclusively by its oxygen atom. Interestingly, owing to the chiral space group $P2_12_12_1$, the (*R*)-(+)-MTSO ligand makes the entire lattice helical. According to the crystallographic results on $[Ln(C_5H_5)_3 \cdot MTSO]$ systems currently available (see Table 1), all members of this particular class from La to Yb seem to be isostructural.

The three new indenyl complexes **1b**, **2a** and **2b** are isostructural with, but not always equally configured as, the earlier reported[10] complex **1a**, so that **1a** and **1b**, and the pair **2a** and **2b** can be considered as genuine optical antipodes (Figure 2). In accordance with the polarity of the S=O bond, the Ln–O distances of all sulphoxide adducts investigated are significantly shorter than those of the corresponding THF adducts (Table 2). From the Ln–O(S) distances listed in Table 2, a slightly shorter Gd–O distance can be extrapolated than actually reported for the novel sulphur dioxide complex $[Gd(SO_2)_3(\mu\text{-}AsF_6)_3]_n$ (243(2)–245(1) pm).[20] The S=O bond is only about 3 pm longer than in noncoordinated MTSO.[21]

Abstract in Chinese: 摘 要

合成与表征了一系列新型稀土亚砜的1:1加成物 [LnCp"$_3$·OSR$^{(1)}$R$^{(2)}$] (Cp" = C_5H_5 或 C_9H_7; R$^{(1)}$/R$^{(2)}$ = Me/4-MeC_6H_4 (MTSO) 或 Ph/Ph (DPSO); Ln = La, Pr, Nd 或 Sm)。固态的 [Ln(C_9H_7)$_3$·MTSO] (Ln = La 或 Pr,) 分子中含有一个以氧原子配位的亚砜基团和三个五配位的茚基。三个茚基的定向取向，使中心金属离子处于手性环境中。但是在溶液中，分子中 (Ln = Pr, Nd 或 Sm) 的茚基基团处于 $\eta^5 \leftrightarrow \eta^1$ 快速振荡之中。随着温度的降低，这一振荡过程有利于向右进行。固二色性和变温核磁共振氢谱的研究表明，由于这一振荡的存在，在离金属离子更近的位置，产生了另一个新的手性中心，由于对原子手性中心的选择性和控制作用，使得这个新的手性中心只对其中某一个构型 (S 或 R) 能够相对稳定的存在。与此相反，尽管Ln-O键长比相应THF加成物短10 pm左右，但环戊二烯基类似物 (Cp = C_5H_5, Ln = Pr, Nd, Yb) 实际上并没有明显的园二色效应。令人吃惊的是，两种 [Ln(C_9H_7)$_3$·MTSO] (MTSO = R-(+)- 或 S-(-)-MTSO, 或两种不同的稀土离子) 混合物的核磁共振波谱的研究发现，亚砜基团不但存在着分子内的偶合–分离过程，而且有着更显著的分子间的相互交换。然而在另一方面，这种分子间的相互交换在MTSO和THF两种配体之间却是不存在的，这说明亚砜基团的分子间交换反应可能是按照某种特殊的途径进行的。

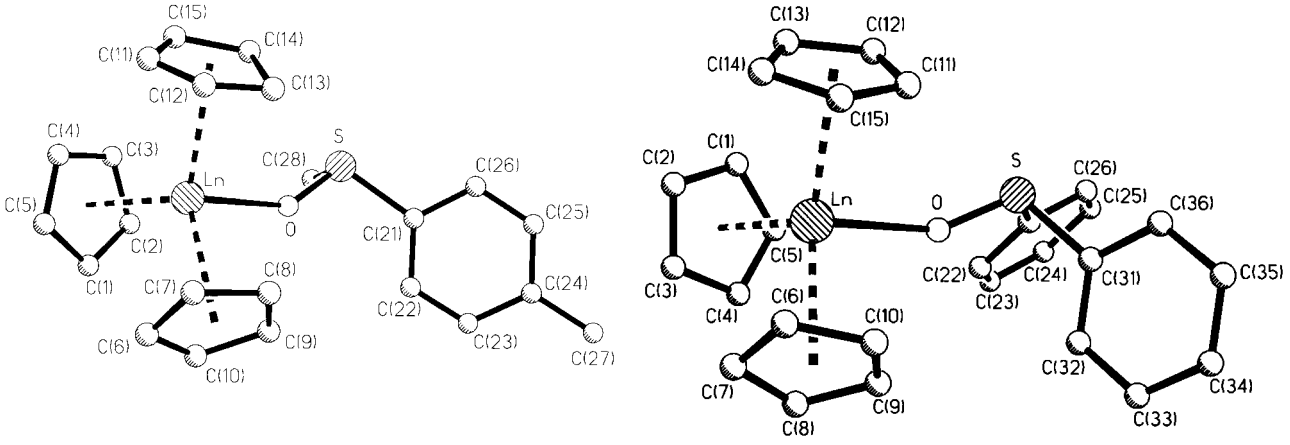

Figure 1. Molecular structures of a) **8a**–**10a** and b) **13** and **14**, including the atomic numbering schemes.

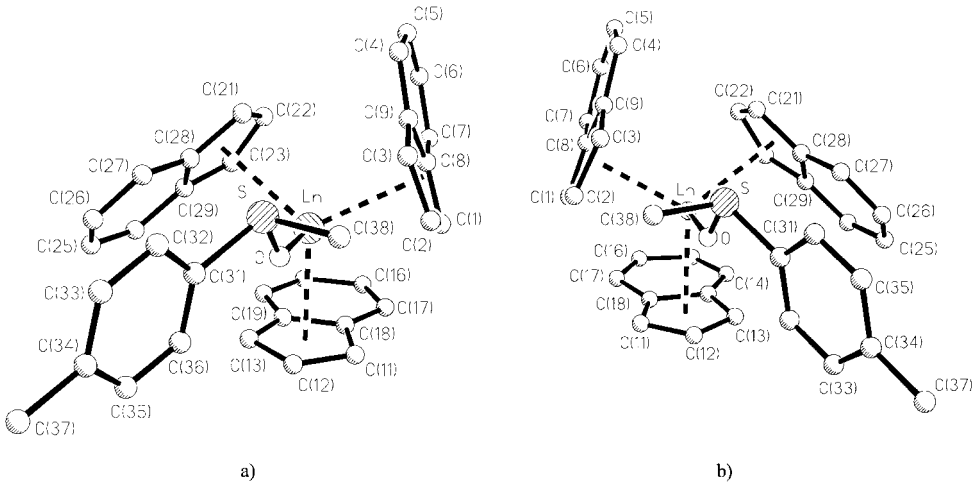

Figure 2. Molecular structures of a) **1a** and **2a** and b) **1b** and **2b**, including the atomic numbering schemes.

As we have stated earlier,[10] the chiral sulphoxide ligand helps to generate a chiral $\{Ln(C_9H_7)_3O\}$ fragment as a result of a specific disposal of each of the benzo groups of the three indenyl ligands. While one benzo group lies approximately *transoid* to the Ln–O vector, the orientation of the other two is reminiscent of a paddle wheel with two paddles and the Ln–O bond as axis. As the two paddles are oriented counter-clockwise in the presence of (*R*)-(+)-MTSO, but clockwise in the presence of (*S*)-(−)-MTSO (Figure 2), each of the four complexes **1a**, **1b**, **2a** and **2b** contains *two* distinct stereogenic centres. So far, we have not observed any of the two diastereomers of the combinations: clockwise/(*R*)-(+) and anti-clockwise/(*S*)-(−). The actual disposal of each of the indenyl ligands may be further quantified by consideration of the shortest individual distances D_n ($n = 1-3$) from the centre of each benzo group to the plane spanned by the centres of the three five-membered ring fragments of the indenyl ligands[5, 6] (Table 3). For ideal paddle-wheel-like arrangements, the D_n values should approach zero (but ca. 220 pm for an ideal meridional arrangement). From the data in Table 3, it is apparent that the centres of the benzo groups of the paddle-like indenyl ligands of **1** and **2** reside alternately above and below the reference plane (above is defined as *cisoid* to the metal ion). Table 3 also includes the D_n values of the related DPSO adduct **7** with Ln = Nd. For comparison, base-free $[Pr(C_9H_7)_3]$ with three *cisoid*–meridional and $[Sm(C_9H_7)_3 \cdot THF]$ with three equatorial indenyl ligands are also considered. Obviously, the data set of **7** differs from the sets of **1** and **2**, since the three paddles are almost equally distorted from the ideal paddle-wheel arrangement. Although **7** contains no *chiral* sulphoxide, the $\{Nd(C_9H_7)_3O\}$ fragment could, strictly speaking, be considered as chiral. The structure of **7** in the crystal involves a racemic mixture of molecules with respect to the new chirogenic centre; the molecular structure of one enantiomer of **7** is shown in Figure 3.

Table 3. Comparison of the parameters D_n and Δ_n [pm] of the title complexes and base-free $[Pr(C_9H_7)_3]$.[a]

	C_9H_7 (1)		C_9H_7 (2)		C_9H_7 (3)		Ln–PL
	D_1	Δ_1	D_2	Δ_2	D_3	Δ_3	
1a	−159.8	17.3	−216.2	3.3	143.6	13.8	39.3
1b	−158.8	17.0	−215.9	3.7	144.1	13.2	39.7
2a	−159.2	18.6	−217.4	1.8	140.7	13.1	38.1
2b	−158.9	19.4	−216.6	4.1	142.5	14.3	38.5
7	141.8	14.6	111.2	16.7	127.2	16.1	49.2
$[Pr(C_9H_7)_3]$[6]	197.7	4.4	210.5	1.7	195.0	5.0	21.1
$[Sm(C_9H_7)_3 \cdot THF]$[6]	25.6	7.1	25.6	7.1	25.6	7.1	52.3

[a] $\Delta = \langle Ln–C(8,\ 9)\rangle_{av} - \langle Ln–C(1,\ 2,\ 3)\rangle_{av}$; Ln–PL = shortest distance between Ln and the plane spanned by the three C_5 centres of the indenyl ligands. The numbering of the C_9H_7 ligands follows that chosen for Figures 2 and 3. For the sign of D_1 and D_2 see the text.

In all five indenyl complexes considered here (**1a/b**, **2a/b** and **7**) the two C_9H_7 carbon atoms shared by the C_5 and the C_6 fragment of each indenyl group are slightly more distant from the metal ion than the other three C_5 carbon atoms. This quite general feature is documented for the title compounds and for some related complexes (Table 3). We have correlated the

0947-6539/99/0507-1994 $ 17.50+.50/0 *Chem. Eur. J.* **1999**, *5*, No. 7

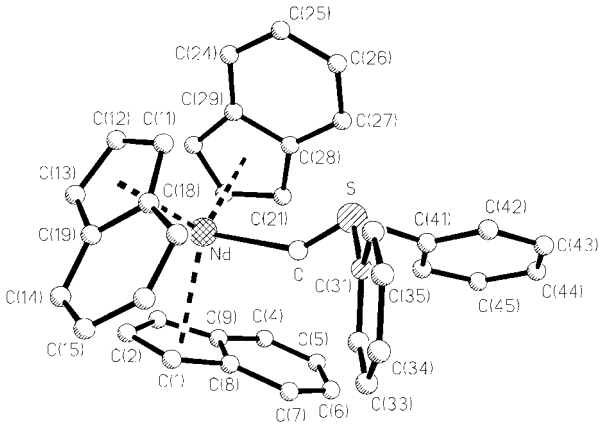

Figure 3. Molecular structure of **7** with the atomic numbering scheme.

quite frequent inequality of the Ln–C bond lengths of indenyl complexes with the variable steric congestion dependant on the spatial disposition of each C_9H_7 unit.[6] Instead of rejecting the idea of genuine η^5-bonding, it seems to be more appropriate to talk of only moderately distorted η^5-coordination.

Room-temperature ^{1}H NMR spectra of single indenyl complexes: All complexes examined give rise to solution ^{1}H NMR spectra consistent with the presence of three virtually *equivalent* C_5H_5 or C_9H_7 ligands. While the DPSO adducts **6** and **7** display, as already observed for **5**[10] and various THF adducts,[5] four C_9H_7 proton resonances ($I_{rel} = 6{:}6{:}6{:}3$), the MTSO adducts **1**–**4** give rise to seven equally intense ($I_{rel} = 3$) C_9H_7 signals. The spectrum of diamagnetic **1a** has been reported previously,[10] and so only the room-temperature spectra of three paramagnetic complexes are depicted in Figure 4. Obviously, enantiomeric pairs of adducts with the

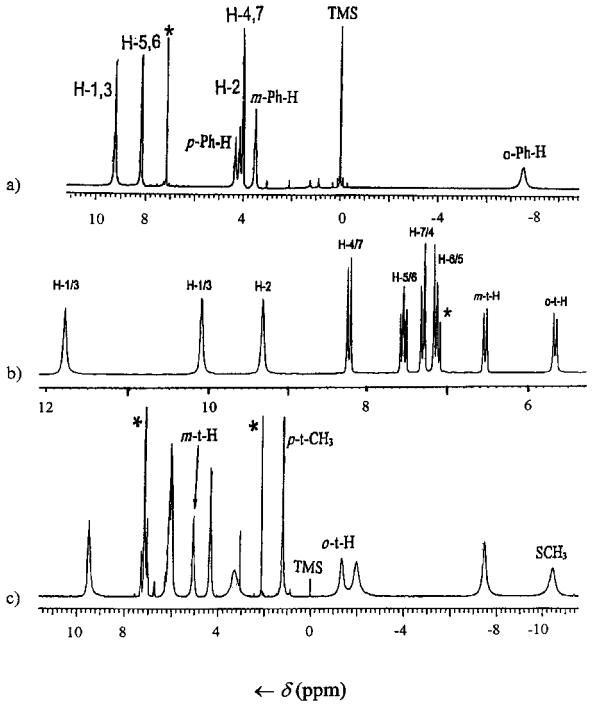

Figure 4. Room-temperature ^{1}H NMR spectra of a) **6** dissolved in [D_8]toluene, b) **4a** in [D_6]benzene and c) **3a** in [D_6]benzene. The methyl proton resonances of **4a** have been omitted. * = solvent.

same central metal, but either (*R*)-(+)- or (*S*)-(−)-MTSO, will have identical spectra. As we have already suggested,[10] the appearance of *seven* signals could be due to the prochiral nature of the indenyl proton pairs H1/3, H4/7 and H5/6 of each {Ln(η^n-C_9H_7)} fragment ($n = 3$ or 5), the resonances of which would undergo diastereotopic splitting as soon as another ligand (such as chiral MTSO) introduces a stereogenic centre (see Figure 5). The actual observation of

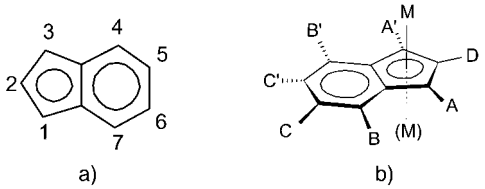

Figure 5. a) Conventional numbering of indenyl hydrogen atoms. b) Schematic description of the prochiral nature of the atoms A/A′, B/B′ and C/C′ in a {M(η^n-indenyl)} fragment. A change of the coordinated face (i.e., M → (M)) would convert the unprimed atoms to primed atoms and vice versa.

diastereotopic splitting rules out any rapid (on the NMR time scale) intra- or intermolecular scrambling capable of interconverting the coordinated face of a C_9H_7 ligand. Such a process would destroy the prochiral nature by quenching all diastereotopic splitting.

The observed equality of all three indenyl ligands is therefore either caused by rapid intramolecular ring mobililty or a rigid, C_3-symmetric fixation of all three indenyl ligands with paddlelike benzo groups. The absence of *two* nonequivalent sets of C_9H_7 and MTSO resonances in any of the recorded spectra, which would be caused by two diastereomers, disfavours the latter view. Although two diastereomers are, in principle, expected, owing to the generation of a second stereogenic centre at the metal site, they might be too shortlived to be observed in solution. It should be recalled that various kinds of chiral {Ln(C_9H_7)$_3$O} fragments have actually been found in the solid state (vide supra), including those with *three* paddle-wheel-like C_9H_7 ligands.[5]

Owing to the well-documented,[22] pronounced absence of substantial NMR line broadenings and line displacements in the paramagnetic $4f^5$ Sm^{III} system, a satisfactory assignment of the seven C_9H_7 proton resonances of **4a** and **4b** is possible (Figure 4 and Table 4). Each of the seven C_9H_7 resonances has retained its specific multiplet pattern. Moreover, in accordance with the expectation that protons of the C_5 fragment should always be affected most strongly by the paramagnetism as they lie closest to the metal ion, the absolute values of the so-called isotropic shift, $|\Delta^{iso}| = |\delta^{para} - \delta^{dia}|$, of **4a** ($\delta^{dia}$ refers to the corresponding chemical shifts of the diamagnetic La complexes **1a**/**b**) are found to decrease in the order: H1/3 > H3/1 > H2 > H4/7 > H5/6 ≫ H6/5, H7/4.

While the C_9H_7 resonances of **3a/b** cannot be reliably attributed to distinct H atoms, because seven equally intense singlets appear, the C_9H_7 resonances of **2a/b** can be plausibly assigned (Table 4). There is little uncertainty in view of the four signals that display low $|\Delta^{iso}|$ values and pairs of doublet and triplet patterns, but some ambiguity remains for the two singlets with $\Delta^{iso} = -6.47$ and -4.46 pm. One of them should

Table 4. Comparison of the proton resonance patterns of selected indenyl complexes and binary mixtures thereof, including the isotropic shifts Δ^{iso} of **2a** and **4a**.[a]

	Complex	Resonances of indenyl protons H-1,3	H-2	H-4,7	H-5,6	Resonances of MTSO/DPSO protons *m*-tolyl-H	*o*-tolyl-H	*p*-tolyl-CH_3	SCH_3
La	**1a**	5.81(s)	6.44(t)	7.32(d)	6.93(t)	6.84(d)	7.00(d)	1.80(s)	1.94(s)
		6.14(s)		7.66(d)	7.01(t)				
La	**1a**+**1b** (1:1)	5.97(d)	6.42(t)	7.50(q)	7.0(q)	6.83(d)	6.95(d)	1.75(s)	1.94(s)
Sm	**4a**	10.08(s)	9.34(s)	7.30(d)	7.15(t)	6.52(d)	5.64(d)	1.79(s)	0.01(s)
		11.79(s)		8.24(d)	7.56(t)				
	Δ^{iso}, **4a**	+4.11	+2.90	−0.19	+0.18	−0.48	−1.20	−0.01	−1.93
		+5.82		+0.75	+0.59				
	4a+**4b** (1:1)	10.95(s)	9.36(s)	7.67(s)	7.67(s)	6.56(d)	5.66(d)	1.83(s)	0.11(s)
Pr	**2a**	19.55(s)	1.98(s)	10.41(d)	4.95(t)	4.18(s)	−5.86(s)	0.87(s)	−13.30(s)
		−0.52(s)		6.22(d)	3.85(t)				
	Δ^{iso}, **2a**	+13.68	−4.46	+2.92	−2.02	−2.66	−12.86	−0.93	−15.24
		−6.47		−1.27	−3.12				
Pr	**2a**+**2b** (1:1)	absent		1.83(s)	8.52(s)	4.17(s)	4.17(s)	−5.98(s)	0.5(s)	−13.59(s)
La	**5**	5.97(d)	6.42(t)	7.84(q)	6.90(q)	6.89(m)[b]	7.24(dd)		
Pr	**6**	9.25(s)	4.16(s)	8.18(q)	4.02(dd)	3.51(t)	−7.55(s)	4.34(t)[c]	

[a] All samples were dissolved in C_6D_6, except for the mixtures of (**1a**+**1b**) and (**2a**+**2b**), which were studied [D_8]toluene solution. [b] Involving *m- and p*-phenyl-H. [c] Here of *p*-phenyl-H.

belong to H2, and one to H1/3. More clarity will be provided in the following paragraphs.

Room-temperature ^{1}H NMR spectra of binary mixtures of indenyl complexes. In the absence of any *rapid* intermolecular exchange of sulphoxide ligands, the ^{1}H NMR spectra of solutions that contain two different adducts should not deviate from the simple superposition of the individual spectra. However, exact 1:1 mixtures of **1a** and **1b** were found to give rise to a spectrum devoid of any diastereotopic splitting, as observed for the achiral complex **5**,[10] in which no more than four distinct multiplets can be ascribed to the seven indenyl protons (see Table 4). Solutions of mixtures with **1a**/**1b** ratios slightly different from 1.0 afford continuously modified spectra, in agreement with a rapid, concentration-dependent exchange equilibrium. Correspondingly, the ^{1}H NMR spectra of the freshly prepared, quasi-racemic 1:1 mixtures of **3a**/**3b** or **4a**/**4b**, display only four indenyl resonances instead of seven.

Exact 1:1 mixtures of the paramagnetic quasi-enantiomers **2a** and **2b** display, in addition to three signals unambiguously attributable to MTSO protons, three singlets of different intensity and line width (Figure 6 and Table 4). At a **2a**/**2b** ratio of 1.2, the broad resonance at lowest field splits into two signals and the neighbouring intense signal into three signals. The relatively weak new doublet should belong to the *m*-tolyl protons of the MTSO ligand. At a **2a**/**2b** ratio of 16:1, two more signals emerge at about $\delta = 19$ and -0.5, and as the **2a**/**2b** ratio is raised further, the NMR spectra approach the appearance of the room-temperature spectrum of pure **2a** or **2b**. The systematic examination of the ^{1}H NMR spectra for different **2a**/**2b** ratios thus confirms that, owing to their pairwise collapse at a **2a**/**2b** ratio of 1:1, the two doublets at $\delta = 6.22$ and 10.41 and the two triplets at $\delta = 3.85$ and 4.95 of pure **2a** (or **2b**) belong to prochiral pairs of C_9H_7 protons. Moreover, the two widely separated, but nevertheless coalescing, singlets (at $\delta = -0.52$ and 19.55) should be assigned to H1 and H3. The remaining singlet of pure **2a**/**b** at $\delta = 1.98$, which is easily detected at all **2a**/**2b** ratios, would then be best ascribed to H2. The well-reproducible, complete breakdown of the diastereotopic splitting of all C_9H_7 resonances in the racemic 1:1 mixtures contrasts with the persistence of all signals of the MTSO protons. Both features can, however, be rationalized in terms of continuous and rapid, *inter*molecular exchange of (*R*)-(+)- and (*S*)-(−)-MTSO ligands. This view is well-supported by the observation that a 1:1 mixture of diamagnetic **1a** and paramagnetic **2a** gives rise to a significantly perturbed resonance pattern of the MTSO protons (Figure 7a), while the C_9H_7 resonances still correspond to those of pure **1a** and **2a**. The (*R*)-(+)-MTSO molecules oscillate rapidly between diamagnetic and paramagnetic metal centres, leading, inter alia, to considerable broadening or even the

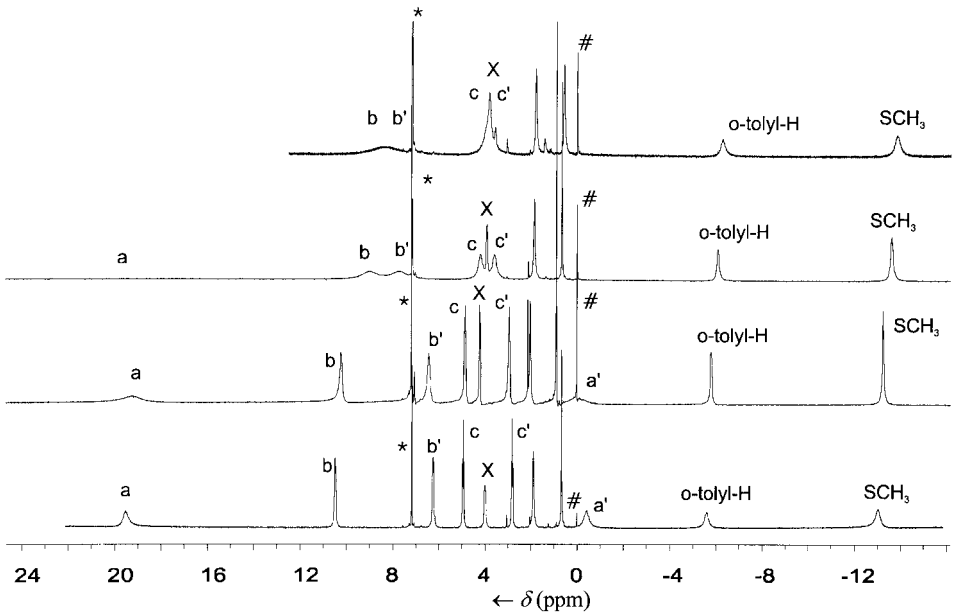

Figure 6. ^{1}H NMR spectra of (from top to bottom): a 1:1 mixture, a 1.2:2 mixture and a 16:1 mixture of **2a** and **2b**, and pure **2a**. The designations a/a′, b/b′ and c/c′ correspond to the C_9H_7 proton pairs H1/3, H4/7 and H5/6. Solvent: [D_6]benzene. X = m-tolyl-H, # = TMS, * = solvent.

0947-6539/99/0507-1996 $ 17.50+.50/0 *Chem. Eur. J.* **1999**, *5*, No. 7

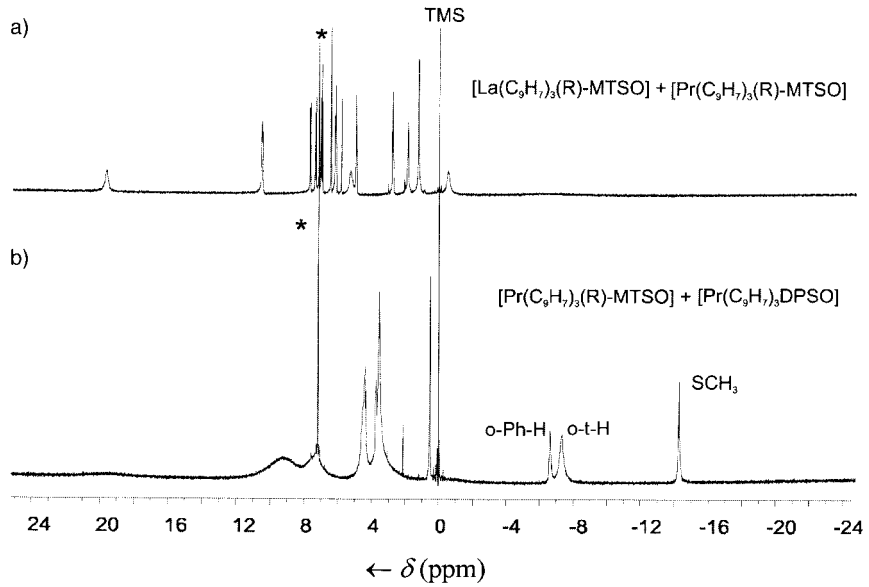

Figure 7. ^{1}H NMR spectra of 1:1 mixtures of a) **1a** and **2a** and b) **2a** and **6**. Solvent: [D_6]benzene. * = solvent.

disappearance of MTSO signals. Evidently, equally rapid, although undetectable, *inter*molecular sulphoxide exchange must also be assumed to occur in the solution of a *pure* tris(indenyl)lanthanoid complex carrying a sulphoxide ligand.

In a related experiment, the ^{1}H NMR spectrum of a 1:1 mixture of **1b** [with (*S*)-(−)-MTSO] and **2a** [with (*R*)-(+)-MTSO] was inspected. As before, the resonances of the MTSO protons were strongly affected while, owing to the involvement of both MTSO enantiomers, the La-bonded C_9H_7 ligands gave rise to only four multiplets and the Pr-bonded C_9H_7 ligands to no more than three comparatively broad singlets (vide supra). More surprisingly, a 1:1 mixture of **2b** (chiral) and **6** (achiral) that should display a total of eleven signals in the absence of any exchange, actually gave rise to no more than four C_9H_7 resonances (Figure 7b). As both complexes contain Pr^{III}, the resonances of both sulphoxides remained almost unperturbed. Here again, the experimental results confirm rapid MTSO/DPSO exchange. MTSO exchange also takes place between the indenyl complex **2b** and the cyclopentadienyl complex **8a**, as again the diastereotopic splitting of the C_9H_7 resonances is quenched, and MTSO signals undergo significant perturbation.

In striking contrast to the constantly facile exchange of sulphoxide ligands (vide supra), a corresponding mutual replacement of MTSO by THF molecules (and vice versa) seems to be inhibited. Thus, solutions of the mixtures **1a**/[$La(C_9H_7)_3 \cdot THF$] and **2b**/[$Pr(C_9H_7)_3 \cdot THF$] gave rise, for various molar ratios, only to the clean superpositions of the ^{1}H NMR spectra of the pure components. It should be recalled that, according to crystallographic results (see Table 2), the Ln–O(THF) distance always exceeds the Ln–O(SR_2) distance; this anticipates an even better mobility of the THF molecules. This expectation has experimentally been confirmed for 2-methyltetrahydrofuran (MeTHF), since solutions of [$Pr(C_9H_7)_3 \cdot$ *rac*-MeTHF] displayed exclusively *four* C_9H_7 proton resonances between 50 and −70 °C.[23] An unexpected mechanistic scenario emerges from these observations in which rapid MTSO exchange would take place exclusively between MTSO adducts in the same solution and, independently, rapid THF exchange exclusively between THF adducts. Some doubt might thus arise in the presence of ideally separated, strictly mononuclear complexes in the otherwise strictly homogenous solution.

^{1}H VT-NMR spectra of single indenyl complexes. In view of the frequently observed proportionality of the chemical shifts of paramagnetic samples and the reciprocal temperature, all VT-NMR results have been presented graphically by the corresponding δ versus T^{-1} diagrams. First of all, the divergence of distinct pairs of δ versus T^{-1} curves, which includes the *diamagnetic* complex **1a** (see Figure 8a), suggests that the amount of diastereotopic split-

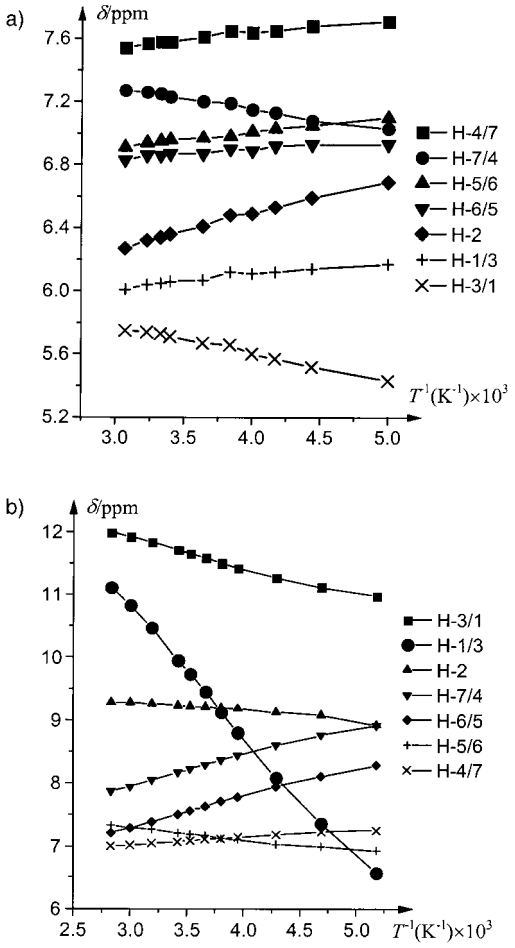

Figure 8. Comparison of the δ versus T^{-1} diagrams of the C_9H_7 proton resonances of a) **1b** and b) **4a**. Solvent: [D_8]toluene.

ting increases with decreasing temperature; this reflects, inter alia, a concomitantly longer lifetime of the adduct. A corresponding trend is found for the moderately paramagnetic complex **4a**; here the diastereotopic splitting is rapidly magnified by the temperature dependence of the magnetic susceptibility of the Sm^{III} ion (Figure 8b). More surprisingly, the δ versus T^{-1} plots of the indenyl protons H1 and H3 of **4a** show an *inverse* temperature dependence: although the positive isotropic shifts Δ^{iso} of these nuclei should further increase if the Curie–Weiss law is obeyed, the two Δ^{iso} values decrease significantly with decreasing temperature. The slope of that particular δ versus T^{-1} plot differs drastically from all other curves including the plots of the MTSO protons (Figure 9a). This feature raises the question of whether the

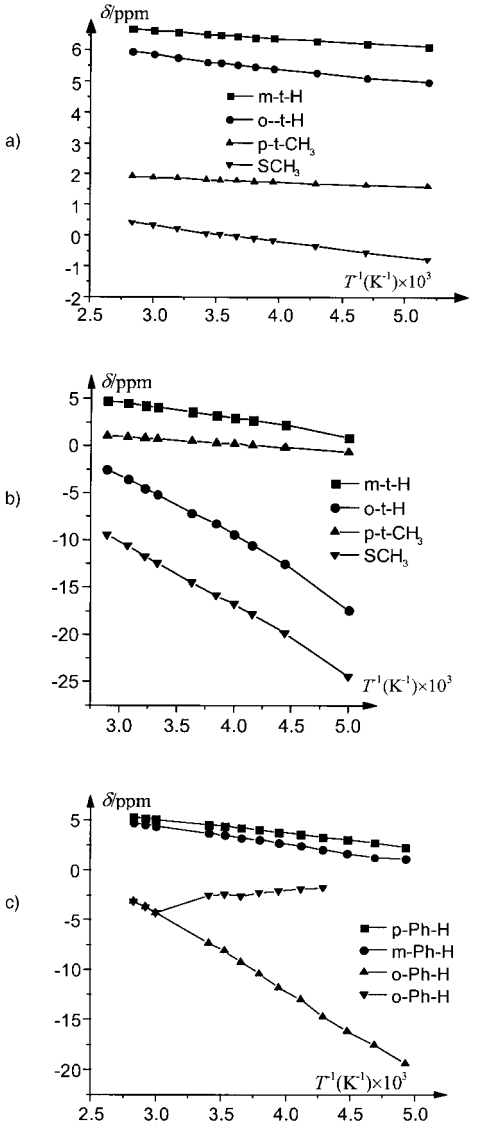

Figure 9. Comparison of the δ versus T^{-1} diagrams of the sulphoxide protons of a) **4a**, b) **2a** and c) **6**. Solvent: [D_8]toluene.

unusual shift of δ from 11.1 at $+80\,^{\circ}C$ to 6.5 at $-80\,^{\circ}C$ could be caused by corresponding changes of the magnetic susceptibility tensors of the Sm^{3+} ion. Alternatively, a virtually continuous change of the *chemical* nature of the proton in question might be taken into account: generally, any conversion of an aromatic proton into an aliphatic one would lower the ^1H NMR shift by about 3–4 ppm. Corresponding signal displacements are well documented for the NMR spectra of fluxional metal complexes in which a cyclopentadienyl (or indenyl) ligand undergoes interconversion from η^5 to η^1-hapticity.[1, 24, 25] In the case of **4a** and **4b**, the equilibria in Equation (1) could account best for this particular mode of rapid isomerization.

$$[Sm(\eta^5\text{-}C_9H_7)_3 \cdot MTSO] \rightleftharpoons [Sm(\eta^5\text{-}C_9H_7)_2(\eta^1\text{-}C_9H_7) \cdot MTSO] \rightleftharpoons \ldots \quad (1)$$

The virtual equivalence of all three indenyl ligands (vide supra) requires that each of them adopt η^1-hapticity with the same probability and that the all-η^5-isomer becomes less abundant with decreasing temperature. Provided that the coordinated C_5 face does not change (vide supra), each of the C_9H_7 ligands can generate a racemic pair of {Ln(η^1-C_9H_7)} fragments, in which the otherwise equivalent, σ-bonded (to Ln) and chiral ring carbon atoms C1 and C3 become optical antipodes. In the presence of only *one* MTSO enantiomer, two diastereomers of different steric congestion should result. However, the VT-NMR spectra of **1**–**4** are devoid of any evidence of two isomers, which lends strong support to just one particular diastereomer. Steric congestion is indicated by the emergence of two low-temperature plots for the *o*-phenyl protons of the DPSO ligand of **6** (Figure 9c).

While the complexes **3a** and **3b** (Ln = Nd) also give rise to seven approximately linear δ versus T^{-1} curves for the C_9H_7 protons, any further interpretation would at present remain rather speculative. On the other hand, from a comparison of the δ versus T^{-1} diagrams of chiral **2b** (Figure 10a) and achiral **6** (Figure 10b), more insight into the fluxional nature the structure of **2a** or **2b** in solution is available. Interestingly, four δ versus T^{-1} plots similar to the four experimental curves of **6** result when, following the assignment proposed for **2a** in Table 4, the values of δ(H2) and the average values of δ(H1)/δ(H3), δ(H4)/δ(H7) and δ(H5)/δ(H6) of **2b** are plotted versus the reciprocal temperature (Figure 10b). The quite successful, tentative simulation of the quenching of the diastereotopic splitting for **2b** not only helps to confirm the earlier proposed assignment, but also supports the view that both **2** and **6** are fluxional in accord with the equilibria indicated by Equation (1). In striking similarity to the δ versus T^{-1} diagram of **4a**, the δ versus T^{-1} diagrams of **2b** and **6** also contain one particular curve (to be ascribed to H1 or/and H3) that surprises by its pronounced high-field shifts with decreasing temperature. Thus, Δ^{iso} of **2b** drops from about $\delta = -3.1$ at $70\,^{\circ}C$ to about $\delta = -40.7$ at $-70\,^{\circ}C$, while Δ^{iso} of **6** changes from $\delta = +3.7$ at $+80\,^{\circ}C$ to $\delta = -2.8$ at $-70\,^{\circ}C$. Hence, as in the case of **4a** (vide supra), the chiral MTSO ligand again dictates the preference of one distinct diastereomer of **2a** or **2b**, whereas the protons H1 and H3 of **6** remain equivalent. A δ versus T^{-1} diagram very similar to that shown in Figure 10a (solvent D_8[toluene]) has also been obtained for **2a** in CD_2Cl_2.

^{1}H VT-NMR spectra of binary systems of indenyl complexes: To determine the temperature range at which the intermolecular exchange of MTSO molecules slow down on the NMR

0947-6539/99/0507-1998 $ 17.50+.50/0 *Chem. Eur. J.* **1999**, *5*, No. 7

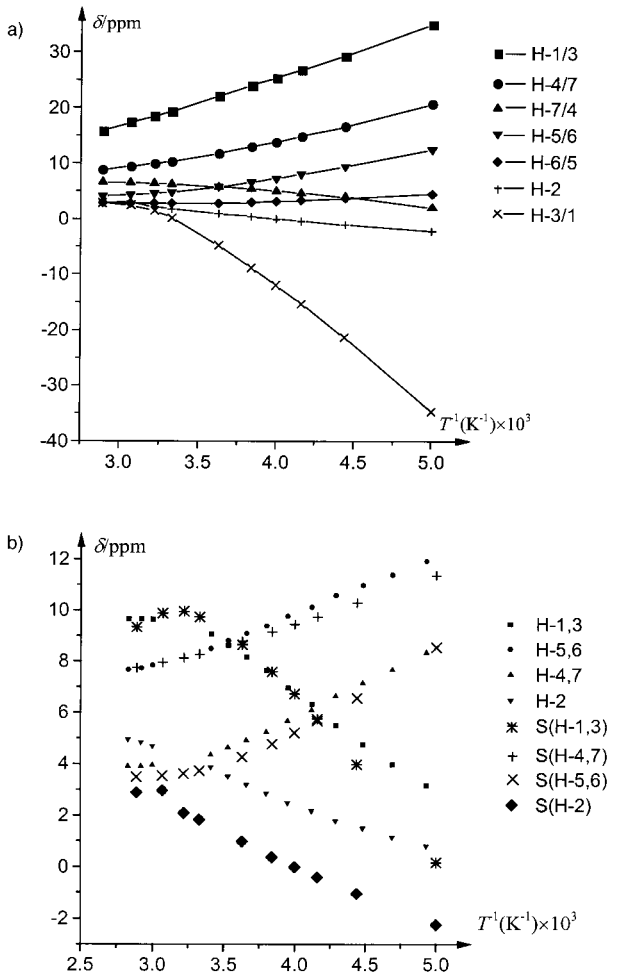

Figure 10. Comparison of the δ versus T^{-1} diagrams of the C_9H_7 protons of a) **2b** and b) **6**. Experimental data points for **6** are depicted by smaller symbols, while the larger symbols designated by an S refer to simulated δ versus T^{-1} curves (see text). Solvent: [D_8]toluene.

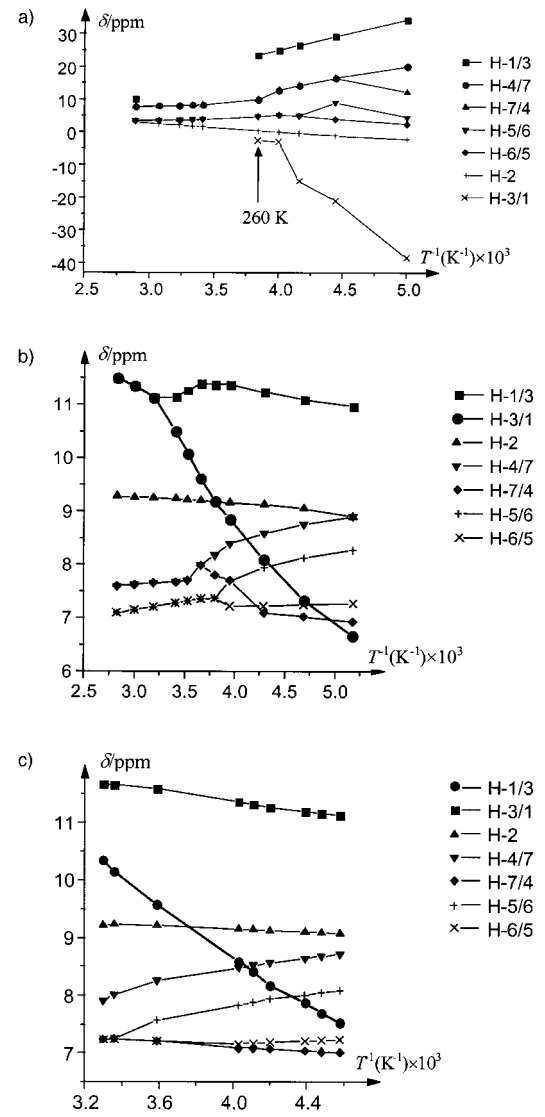

Figure 11. δ versus T^{-1} diagrams of a) a 1:1 mixture of **2a** and **2b**, b) a 1:1 mixture of **4a** and **4b** immediately after the preparation of the sample and c) 23 days later. Solvent: [D_8]toluene.

time scale, the ^{1}H NMR spectrum of a 1:1 mixture of **2a** and **2b** dissolved in [D_8]toluene was also inspected in the temperature range $+70$ to $-70\,^\circ$C. As is seen from the corresponding δ versus T^{-1} diagram (Figure 11a), the curves of the three C_9H_7 resonances detectable at room temperature display reasonably straight lines down to about $-10\,^\circ$C, whereafter a stronger deviation from linearity and a splitting into two branches (i.e., of H1 and H3) occurs. Moreover, between about -30 and $-40\,^\circ$C, the two δ versus T^{-1} curves of H4/7 and H5/6 also undergo the expected splitting. Thus, below about $-40\,^\circ$C, a seven-line pattern is again obtained; this indicates that each adduct molecule has become sufficiently long-lived.

A notably different situation is found for the solution of a **4a**/**4b** (1:1) mixture. While the δ versus T^{-1} diagram recorded immediately after the preparation of this solution (Figure 11b) still resembles that obtained for the **2a**/**2b** mixture (Figure 11a) in that seven curves emerge from initially four quasi-linear plots at lower temperatures only, the appearance of the δ versus T^{-1} diagram of the same solution (in a sealed tube) changed drastically with time. After 23 days, a diagram of the somewhat intermediate appearance shown in Figure 11c was obtained, and the δ versus T^{-1} diagram recorded 38 days after the preparation of the solution looked practically identical with that found for solutions of pure **4a** (Figure 8b). Hence, the finally studied sample formally appears to involve molecules that do not exchange (*R*)-(+)-MTSO molecules against their (*S*)-(−)-enantiomers and vice versa. This situation is somewhat reminiscent of the inhibited mutual exchange of MTSO and THF molecules (vide supra).

^{139}La NMR spectroscopy: In excellent agreement with the expectation that the total ligand hapticity of the fluxional [$Ln(C_9H_7)_3 \cdot$MTSO] systems [Eq. (1)] should in average be lower than for related rigid molecules with three strictly η^5-coordinated Cp ligands, a ^{139}La NMR shift of $\delta = -450$ (in toluene, 45 °C, $W_{1/2} = 2480$ Hz) was found for **1b**. In contrast, a δ (^{139}La) value of -563 (toluene, 25 °C, $W_{1/2} = 390$ Hz) was obtained for the cyclopentadienyl congener **8a**. A δ (^{139}La) value of -558.6 consistent with an all-η^5-hapticity has already been reported for [$La(C_9H_7)_3 \cdot$ THF].[4]

Circular dichroism of f–f ligand-field excitations: According to the assessment of the ^{1}H NMR spectra of the principally chiral pairs of the MTSO adducts **2a/b** and **4a/b**, only one of the two potential diastereomers of the type [Ln(η^5-C_9H_7)$_2$(η^1-C_9H_7)·(*R*)-(+)-MTSO] should be present, although, owing to rapid equilibria [Eq. (1)], its lifetime should be very short. In this particular isomer, the σ-bonded (to Ln) indenyl carbon atom (C1) will be a new chirogenic centre. Being immediately adjacent to the Ln^{3+} ion, this chirogenic centre should be able to influence the 4f electrons of the metal more strongly than the chiral sulphur atom of the MTSO ligand, which is separated from the metal ion by *two* subsequent chemical bonds and should, moreover, be disfavoured by the rapid intermolecular exchange of the MTSO ligand.

To confirm the hypothesis of a new chirogenic centre adjacent to the Ln^{3+} ion independently, we carried out CD[26] studies of [Pr(C_5H_5)$_3$·MTSO] (**9a**) and [Pr(C_9H_7)$_3$·MTSO] (**2a/b**) solutions in the optical f–f excitation ranges $^3H_4 \rightarrow {}^3P_{0-2}$ and $^3H_4 \rightarrow {}^1D_2$ of the system Pr^{III}. Owing to the much shorter time scale of optical spectroscopy, any Cotton effects of the (on the slower NMR time scale) very short-lived isomeric forms of interest should be readily observable. While pure **9a** (see Figure 1a) may be considered as an almost ideal example of a $4f^2$ system subjected exclusively to usually weak, *vicinal* perturbations[27] (which are due to one single chiral atom in the ligand sphere), the isomers of **2a** and **2b**, which are proposed to have one chiral η^1-C_9H_7 ligand and (*R*)-(−)- or (*S*)-(−)-MTSO, are more likely to experience so-called *configurative* perturbations[27] of the f electrons, which are capable of inducing considerably stronger chiroptic (i.e., CD) effects than purely *vicinal* perturbations.

According to the room-temperature CD studies carried out on **9a**, **2a** and **2b**, the f electrons of the cyclopentadienyl complex **9a** display extremely poor chiroptic responses. Under optimized scanning conditions, no more than two very weak signals at 497 nm ($\Delta\varepsilon_m = +1.1 \times 10^{-4}$ L mol^{-1}cm^{-1}) and 482 nm ($\Delta\varepsilon_m = -1.3 \times 10^{-4}$ L mol^{-1}cm^{-1}) could be observed. The homologues **11a** and **12a** of **9a** (Table 1) did not display any detectable chiroptic response at room temperature (i.e., $\Delta\varepsilon_m < 10^{-5}$ L mol^{-1} cm^{-1}), although Yb^{III} should be one of the chiroptically most sensitive 4f systems.[28] In striking contrast, the CD spectra between 400 and 650 nm of **2a** and **2b** consist of at least ten well-shaped signals with $\Delta\varepsilon_m$ values exceeding those of **9a** by more than one order of magnitude (Table 5 and Figure 12). Somewhat smaller $\Delta\varepsilon_m$ values were also observed in CH_2Cl_2 solution. It is, moreover, remarkable that the

Table 5. Regular absorption and circular dichroism data of [Pr(C_9H_7)$_3$·(*R*)-(+)-MTSO] **2a** between 16100 and 21800 cm^{-1}.

E [cm^{-1}]	ε_{mol}[a] [L mol^{-1} cm^{-1}]	CD [cm^{-1}]	$\Delta\varepsilon_{mol}$[a] [$\times 10^4$ L mol^{-1} cm^{-1}]
16108	0.5	16155	−4.2
16247	1.9	–	–
16316	1.8	16313	8.5
16434	2.2	–	–
16549	1.4	16539	9.1
16650	0.8	–	–
16812	0.2	–	–
19569	2.5	–	–
19802	7.6	19817	−30.6
19972	6.7	20226	16.6
20492	8.0	20429	23.5
20618	7.6	20593	−16.9
20747	8.8	20781	7.4
21097	2.1	20964	−14.8
21645	8.4	21177	1.6
21786	5.9	21758	53.7

[a] $c(Pr^{3+}) = 3.058 \times 10^{-2}$ mol L^{-1} in benzene.

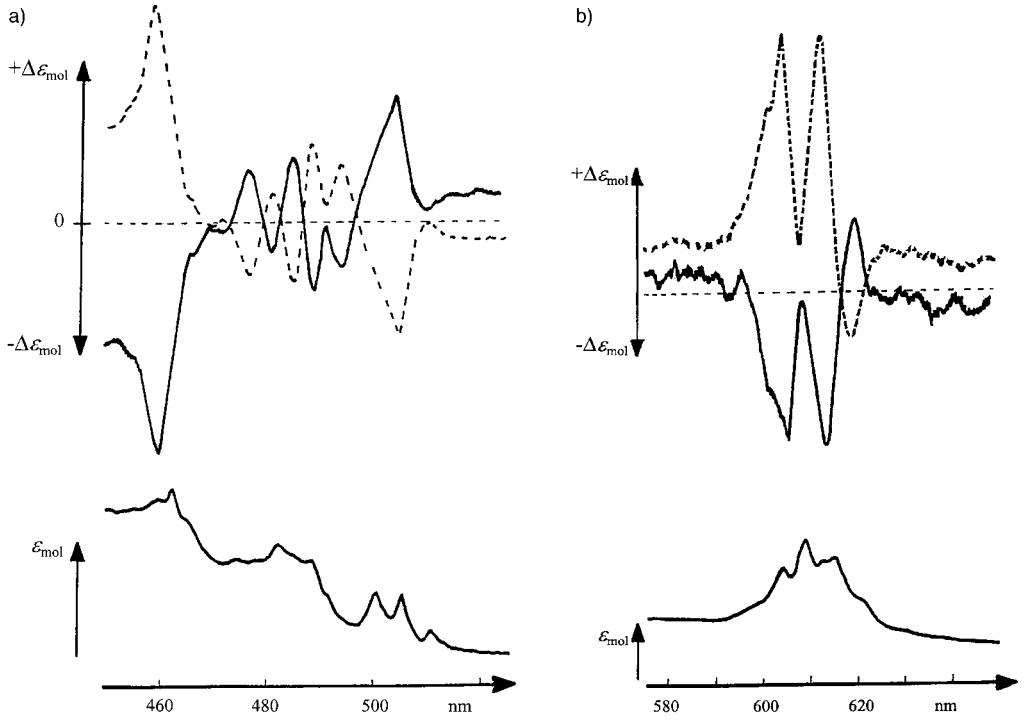

Figure 12. Conventional absorption spectrum (bottom) and f–f CD spectra (top) of **2a** (dotted curve) and **2b** (solid curve) in the ranges: a) 450 to 520 nm and b) 580 to 640 nm. Solvent: benzene.

0947-6539/99/0507-2000 $ 17.50+.50/0 *Chem. Eur. J.* **1999**, *5*, No. 7

indenyl complexes display Cotton effects even for f–f transitions to levels of the ionic $^1D_2$ manifold; these do not, unlike transitions to $^3P_{0-2}$ derived states, belong to the chiroptically more sensitive[28] ionic states of Pr^{III}. In view of the involvement of rapid equilibria (vide supra), which require that only a distinct fraction of all molecules of **2a** or **2b** will be chiroptically active, the absolute $\Delta\varepsilon_m$ values of the most intense Cotton effects are remarkably high. For comparison, the highest $\Delta\varepsilon_m$ values of some appropriately modified tris(β-diketonates) of Pr^{III} with chiral substituents[29] match the largest $\Delta\varepsilon_m$ values of **2a**/**2b**. Similarly, the structurally well-understood organometallic complex [{Pr-(C_5H_5)$_2$$\mu$-{(*R*)-(−)-$OCH_2CHEt(NMe_2)$}}$_2$][30] displays maximal $\Delta\varepsilon_m$ values of $+67.0\times10^{-4}\,L\,mol^{-1}\,cm^{-1}$ (at 22085 cm^{-1}) and of $+18.0\times10^{-4}\,L\,mol^{-1}\,cm^{-1}$ (at 16762 cm^{-1}).[31]

Interestingly, the CD spectra of the indenyl complexes are better resolved than the conventional absorption spectra (Figure 12). As expected for optical antipodes, the CD spectra of **2a** and **2b** display mirror symmetry. Genuine CD peaks are most reliably detectable when the projection of the best mirror plane, which should coincide with the base line, is known. Unfortunately, the high chemical sensitivity of the samples strongly hampered the verification of reproducible concentrations. Results of a first VT-CD experiment for **2b** are shown in Figure 13. Although various experimental deficiencies did not permit sufficiently precise measurements of the actual temperature, and solubility problems did not guarantee the correct knowledge of the true concentrations at lower temperature, the main CD signals of the sample clearly increase as the temperature decreases. Part of this temperature dependence of $\Delta\varepsilon_m$ will be due to the usual temperature dependence of the magnetic susceptibility tensors for magnetic dipole-allowed transitions, but the CD also is expected to increase because the abundance of the species that contain the chiral η^1-C_9H_7 ligand [Eq. (1)] will increase with decreasing temperature.

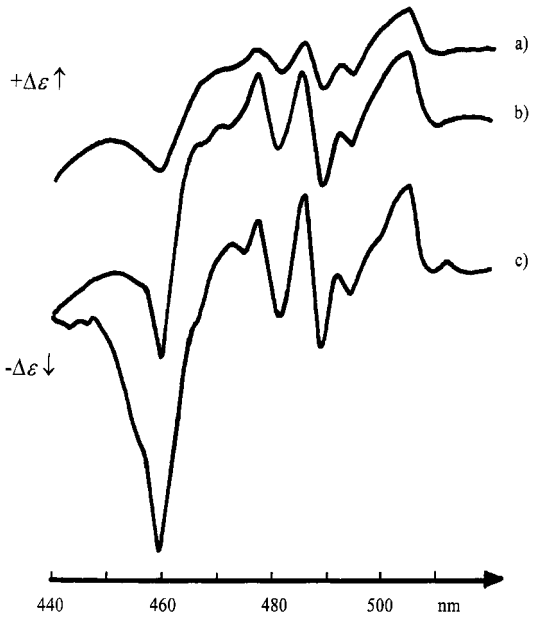

Figure 13. Variable-temperature CD spectrum of a) **2b** at room temperature, b) ca. −30 °C and c) ca. −70 °C. Solvent: toluene.

Conclusions

The results described here clearly demonstrate that isomorphic [Ln(C_9H_7)$_3$ · MTSO] molecules in the crystalline phase do not exist in solution, although both the dissolved and the crystallized molecules involve, in addition to the chiral sulphur atom of the MTSO ligand, a new chirogenic centre close to the metal ion. The presence of the new chiral centre in the dissolved molecules is strongly supported by the NMR results and was independently confirmed by f–f CD spectroscopy. We wish to underline here that satisfactory disentangling of the fluxional nature of the title complexes was only possible by the adoption of *chiral* sulphoxide ligands and, concomitantly, chiroptical studies. Following this strategy, even Evans' interesting hypothesis of η^5/η^1 fluxional [SmCp*$_3$] molecules[3] might successfully be tackled provided that a suitable derivative with a chiral substituent at one ring carbon atom of each Cp* ligand would become available.

In view of the comparatively short Ln−O(MTSO) distances (Table 2), the observation of apparently facile *inter*molecular exchange of sulphoxide molecules is even more striking. Moreover, the surprising inhibition of mutual MTSO/THF exchange suggests that a special mechanism might be responsible for the exclusive exchange of sulphoxide ligands. One first speculation might focus on the formation of contact *pairs* of complexes, in which the sulphoxide ligands would play the role of loose bridges (Figure 14). Such a quasi-symmetrical, short-lived contact pair could, in principle, dissociate in two alternative ways. For instance, from a pair involving the two diastereomers [Ln(η^5-C_9H_7)$_2$(η^1-(*R*)-C_9H_7)(*R*)-(+)-MTSO] and [Ln(η^5-C_9H_7)$_2$(η^1-(*S*)-C_9H_7)(*S*)-(−)-MTSO], alternative diastereomers involving the combinations: (*R*)-η^1-C_9H_7/(*S*)-(−)-MTSO and (*S*)-η^1-C_9H_7/(*R*)-(+)-MTSO could be generated. Nonspontaneous epimerizations could be responsible for some of the still unexplained findings described above. One stable dinuclear complex,[32] faintly reminiscent of the contact pair schematically depicted in Figure 14, involves two Nd^{3+} centres bridged by alkoxide groups and carries two cyclic ether functionalities instead of two η^1-C_9H_7 ligands.

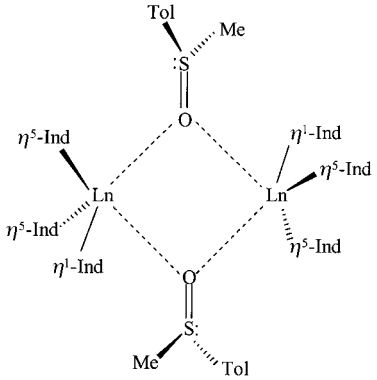

Figure 14. Schematic representation of a potential intermediate responsible for the facile sulphoxide exchange (see text).

Experimental Section

General methods: Manipulation under an inert atmosphere (N_2) was absolutely mandatory. Starting materials and solvents were carefully conditioned as described earlier.[5, 6, 10] Infrared spectra were obtained on

a Perkin–Elmer IR-1720 spectrometer, and NMR spectra either on a Varian Gemini 200 (^{1}H, room temperature) or a Bruker AM 360 spectrometer (^{1}H-VT, ^{139}La). Unless otherwise stated, the samples were dissolved in [D$_6$]benzene for room temperature ^{1}H NMR studies and in [D$_8$]toluene for the VT studies. Solutions for ^{139}La NMR studies were prepared in 3:7 toluene/[D$_8$]toluene, in 10 mm diameter tubes. Standard conditions: deuterium lock, SI = 4 K, TD = 8 K, SW = 71 kHz, DW = 7.0 μs, AQ = 0.05 s, NS = 825. Most of the NMR samples were protected in sealed tubes. Optical (NIR/VIS) absorption spectra were recorded on a Cary 5E instrument, and the f–f CD spectra on a Jasco J 500 G dichrograph equipped with a DP-500 N data processor and a noncommercial low-temperature device. The differential molar extinction values $\Delta\varepsilon_m$ were determined according to ref. [33].

X-ray crystallography: Data collections were performed either on a Hilger–Watts Y 290 diffractometer at 153 K (for crystals of **1b**, **2a**, **2b**, **13** and **14**) or at room temperature (293 K) on a Syntex P2$_1$ instrument (for **7**, **8a**, **9a** and **10a**). Individual crystal data are listed in refs. [11–19]. All measurements were carried out with Mo$_{K\alpha}$ radiation (λ = 70.9261 pm) with the $\omega/2\Theta$-scan technique. All calculations are based on SHELX-93 and SHELXTL-PLUS programme sets.[34] Heavy atoms were found from Patterson maps or located by direct methods, and other non-hydrogen atoms were detected by Fourier techniques. Refinement was based on full-matrix least-squares techniques. Hydrogen atoms were included by use of a riding model with d[C–H] = 96 pm. The absolute configurations of chiral molecules were determined by measurement of the corresponding Friedel pairs (for the individual Flack parameters see refs. [11–13 and 15–17]. $R1 = \Sigma||F_0| - |F_c||/\Sigma|F_0|$; $wR2 = [\Sigma w(F_0^2 - F_c^2)^2]/\Sigma w(F_0^2)^2]^{1/2}$; $S = [\Sigma w(F_0^2 - F_c^2)^2/\Sigma(n-P)]^{1/2}$; $P = [\max(F_0^2,0) + 2F_c^2]/3$. Further details on the crystal structure investigation(s) may be obtained from the Fachinformationszentrum Karlsruhe, D-76344 Eggenstein-Leopoldshafen, Germany (fax: (+49) 7247-808-666); e-mail: crysdata@fiz-karlsruhe.de), on quoting the depository numbers CSD-380176 (**1b**), CSD-380178 (**2a**), CSD-380177 (**2b**), CSD-380175 (**7**), CSD-380183 (**8a**), CSD-380181 (**9a**), CSD-380182 (**10a**), CSD-380180 (**13**) and CSD-380179 (**14**).

Preparation of 1b, 2a, 2b, 3a, 3b, 4a, 4b, 6, 7, 8a, 9a, 10a and 13–15

Synthesis of 1b (also representative for 2a–4b): Under stirring, a solution of (*S*)-(−)-MTSO (Fluka; 0.45 g, 2.97 mmol) in toluene (25 mL) was added to a suspension of [La(C$_9$H$_7$)$_3$·THF][5] (1.65 g, 2.97 mmol) in toluene (20 mL). The mixture soon became a faintly yellow, transparent solution, which was stirred for a further 8 h. After filtration and concentration to a volume of about 8 mL, the solution was cooled overnight at about 0 °C, whereafter the precipitate was collected, washed with hexane (2 × 20 mL) and dried in vacuo. Yield: 1.67 g (88.4%). Recrystallization from hot toluene containing a small amount of THF afforded at 0 °C single crystals of X-ray quality (m.p. 147–150 °C) ^{1}H NMR: see Table 4. C$_{35}$H$_{31}$LaOS (638.60): calcd C 65.86, H 4.85; found: C 65.23, H 4.87%.

Compound 2a: Yield 90%, m.p. 142–145 °C, ^{1}H NMR: see Table 4; C$_{35}$H$_{31}$OPrS (640.60): calcd C 65.65, H 4.84; found: C 65.39, H 4.89%.

Compound 2b: Yield 84.2%, m.p. 146–148 °C; C$_{35}$H$_{31}$OPrS (640.60): calcd C 65.65, H 4.84; found: C 65.63, H 4.96%.

Compound 3a: Yield (after drying at 70 °C): 96%, m.p. 129–132 °C; ^{1}H NMR ([D$_6$]benzene): δ = −10.45 (s, 3H, SMe), −7.46 (s, 3H), −2.0 (s, 3H), −1.35 (s, 2H), 1.20 (s, 3H, *p*-Me), 3.30 (s, 3H), 4.32 (s, 3H), 5.05 (s, 2H), 6.09 (s, 3H), 6.10 (s, 3H), 9.49 (s, 3H); C$_{35}$H$_{31}$NdOS (643.94): calcd C 65.31, H 4.81; found: C 65.96, H 4.91%.

Compound 3b: Yield 78.6%, m.p. 128–130 °C; C$_{35}$H$_{31}$NdOS (643.94): calcd C 65.32, H 4.81; found: C 64.28, H 4.93%.

Compound 4a: Yield 78.0%, m.p. 134–136 °C; ^{1}H NMR: see Table 4; C$_{35}$H$_{31}$OSSm (650.06): calcd C 64.69, H 4.77; found: C 63.99, H 4.91%.

Compound 4b: Yield 80.0%, m.p. 133–136 °C; C$_{35}$H$_{31}$OSSm (650.06): calcd C 64.69, H 4.77; found: C 64.01, H 4.86%.

Synthesis of 7 (also representative for 5[10] and 6): A solution of DPSO (Fluka; 0.52 g, 2.58 mmol) in toluene (20 mL) was added to a suspension of [Nd(C$_9$H$_7$)$_3$·THF][5] (1.45 g, 2.58 mmol) in toluene (30 mL). After stirring the clear solution for 12 h, filtration and concentration of the filtrate to one half of its initial volume, the resulting suspension was left at 0 °C for a few days. Well-shaped, green crystals (1.71 g, 96%; m.p. 197–200 °C) were finally obtained after drying in vacuo at 40–60 °C. ^{1}H NMR ([D$_6$]benzene): δ = −3.87 (s, 6H), −2.14 (d, 4H), −0.89 (s, 3H), 4.75 (t, 4H), 5.12 (s, 6H), 5.23 (t, 2H), 7.66 (s, 6H); C$_{39}$H$_{31}$NdOS (691.98): calcd C 67.72, H 4.48; found: C 67.30, H 4.64%.

Compound 6: Yield 85%, m.p. 196–199 °C; ^{1}H NMR: see Table 4; C$_{39}$H$_{31}$OPrS (691.98): calcd C 68.35, H 4.52; found: C 67.70, H 4.66%.

Synthesis of 8a (also representative for 9a, 10a and 13–15): Under stirring at room temperature (ca. 3 h), a solution of (*R*)-(+)-MTSO (0.22 g, 1.45 mmol) in toluene (20 mL) was added to a suspension of [La(C$_5$H$_5$)$_3$·THF] (0.59 g, 1.45 mmol) in toluene (20 mL). The mixture first became clear and quickly turbid again. After heating almost up to boiling point and quick filtration of the hot solution, the filtrate was slightly concentrated and cooled down slowly (over several days) to room temperature. Colorless needle-shaped crystals were finally collected after washing with cold hexane and drying in vacuo. Yield: 0.62 g (88%); m.p. 226–230 °C; ^{1}H NMR ([D$_6$]benzene): δ = 1.78 (s, 3H, *p*-Me), 1.90 (s, 3H, SMe), 6.23 (s, 15H, C$_5$H$_5$), 6.77 (d, 2H, *m*-Ph), 7.05 (d, 2H, *o*-Ph); C$_{23}$H$_{25}$LaOS (488.42): calcd C 56.58, H 5.12; found: C 56.27, H 5.12%.

Compound 9a: Yield 75%, m.p. 227–231 °C; ^{1}H NMR (CD$_2$Cl$_2$): δ = −20.78 (s, 3H, SMe), −13.73 (s, 2H, *o*-Ph), 2.19 (s, 2H, *m*-Ph), 12.50 (s, 15H, C$_5$H$_5$); ^{1}H NMR ([D$_6$]benzene): δ = −21.75 (s, 3H, SMe), −14.38 (s, 2H, *o*-Ph), −0.45 (s, 3H, *p*-Me), 1.63 (s, 2H, *m*-Ph), 13.30 (s, 15H, C$_5$H$_5$); C$_{23}$H$_{25}$OPrS (490.42): calcd C 56.35, H 5.10; found: C 55.98, H 5.27%.

Compound 10a: Yield 78%, m.p. 226–230 °C; ^{1}H NMR ([D$_6$]benzene): δ = −10.92 (s, 3H, SMe), −4.80 (d, 2H, *o*-Ph), 0.58 (s, 3H, *p*-Me), 2.93 (s, 15H, C$_5$H$_5$), 3.89 (d, 2H, *m*-Ph); C$_{23}$H$_{25}$NdOS (493.76): calcd C 55.98, H 5.06; found: C 55.39, H 5.01%.

Compound 13: Yield 93%, m.p. 227–230 °C; ^{1}H NMR ([D$_6$]benzene): δ = 6.24 (s, 15H, C$_5$H$_5$), 6.86 (m, 6H, *m*-/*p*-Ph), 7.25 (m, 4H, *o*-Ph); C$_{27}$H$_{25}$LaOS (536.47): calcd C 60.47, H 4.66; found: C 59.56, H 4.72%.

Compound 14: Yield 92%, m.p. 230–233 °C; ^{1}H NMR ([D$_6$]benzene): δ = −14.14 (d, 6H, *m*-/*p*-Ph), 1.76 (t, 4H, *o*-Ph), 13.71 (s, 15H, C$_5$H$_5$); C$_{27}$H$_{25}$OPrS (538.47): calcd C 60.25, H 4.64; found: C 59.20, H 4.76%.

Compound 15: Yield 83%, m.p. 235–238 °C; ^{1}H NMR ([D$_6$]benzene): δ = −5.54 (d, 4H, *o*-Ph), 3.08 (s, 15H, C$_5$H$_5$), 3.86 (t, 4H, *m*-Ph), 4.62 (t, 2H, *p*-Ph); C$_{27}$H$_{25}$NdOS (541.80): calcd C 59.88, H 4.61; found: C 59.50, H 4.67%.

Acknowledgements

J.-W.G. would like to express his gratitude to the Friedrich-Ebert-Stiftung (Bonn) for a fellowship. Financial support by the BMBF (Bonn) and technical assistance by Mrs. S. Samba is also greatly appreciated.

[1] a) J. L. Calderon, F. A. Cotton, B. G. DeBoer, J. Takats, *J. Am. Chem. Soc.* **1970**, *92*, 3801, and references therein; b) F. A. Cotton, A. Musco, G. Yagupsky, *J. Am. Chem. Soc.* **1967**, *89*, 6136; c) for more recent reviews on organolanthanoid chemistry see: H. Schumann, J. A. Meese-Marktscheffel, L. Esser, *Chem. Rev.* **1995**, *95*, 865–986; G. Bombieri, G. Paolucci, in *Handbook on the Physics and Chemistry of the Rare Earths, Vol. 25* (Eds.: K. A. Gschneidner, Jr., L. Eyring), Elsevier, Amsterdam, **1998**, pp. 265–413.

[2] W. J. Evans, S. L. Gonzales, J. W. Ziller, *J. Am. Chem. Soc.* **1991**, *113*, 7423.

[3] W. J. Evans, K. J. Forrestal, J. W. Ziller, *J. Am. Chem. Soc.* **1998**, *120*, 9273.

[4] M. Tsutsui, H. J. Gysling, *J. Am. Chem. Soc.* **1968**, *90*, 6880; M. Tsutsui, H. J. Gysling, *J. Am. Chem. Soc.* **1969**, *91*, 3175.

[5] J. Guan, Q. Shen, R. D. Fischer, *J. Organomet. Chem.* **1997**, *549*, 203.

[6] J. Guan, R. D. Fischer, *J. Organomet. Chem.* **1998**, *564*, 167.

[7] a) M. Adam, E. T. K. Haupt, R. D. Fischer, *Bull. Magn. Reson.* **1990**, *12*, 101; b) M. Adam, Ph. D. Thesis, University of Hamburg, **1990**, p. 50.

[8] C. Ni, D. Deng, C. Qian, *Inorg. Chim. Acta* **1985**, *110*, L7; a crystal structure analysis of [Yb(C$_5$H$_5$)$_3$·THF] was only mentioned in passing by W. J. Evans, D. K. Drummond, L. R. Chamberlain, R. J. Doedens, S. G. Bott, H. Zhang, J. L. Atwood, *J. Am. Chem. Soc.* **1988**, *110*, 4983.

[9] a) J. Stehr, Ph. D. Thesis, University of Hamburg, **1993**, pp. 12, 15, 29; b) A Steudel, J. Stehr, E. Siebel, R. D. Fischer, *J. Organomet. Chem.* **1996**, *510*, 197.

  0947-6539/99/0507-2002 $ 17.50+.50/0

[10] J. Guan, R. D. Fischer, *J. Organomet. Chem.* **1997**, *532*, 147.
[11] Crystal structure of [La(C_9H_7)$_3$(S)-(−)-MTSO] (**1b**): $C_{35}H_{31}LaOS$, $M_r = 638.60$, monoclinic, $P2_1$, $a = 836.5(1)$, $b = 963.9(3)$, $c = 1767.0(8)$ pm, $\beta = 90.81(2)^\circ$, $V = 1.4246(8)$ nm^3, $Z = 2$, $\rho_{calcd} = 1.489$ g cm^{-3}, $\mu = 1.599$ mm^{-1}, $F(000) = 644$; total no. of reflections 4636, unique reflections 3808 ($R_{int} = 0.0368$). Data/restraints/parameters: 3712/1/345, Flack parameter: 0.01(3). Final R indices: $R1 = 0.0398$, $wR2 = 0.0915$ on data with $I \geq 4\sigma(I)$ and $R1 = 0.0669$, $wR2 = 0.2356$ on all data, goodness-of-fit $S = 1.077$; largest difference peak and hole: 1372 and −1028 e nm^{-3}.
[12] Crystal structure of [Pr(C_9H_7)$_3$(R)-(+)-MTSO] (**2a**): $C_{35}H_{31}OPrS$, $M_r = 640.60$, monoclinic, $P2_1$, $a = 831.0(2)$, $b = 954.6(2)$, $c = 1752.5(5)$ pm, $\beta = 91.51(2)^\circ$, $V = 1.3897(6)$ nm^3, $Z = 2$, $\rho_{calcd} = 1.531$ g cm^{-3}, $\mu = 1.855$ mm^{-1}, $F(000) = 648$; total no. of reflections 2102, unique reflections 1606 ($R_{int} = 0.0246$). Data/restraints/parameters: 1606/1/345, Flack parameter: −0.02(3). Final R indices: $R1 = 0.0302$, $wR2 = 0.0744$ on data with $I \geq 4\sigma(I)$ and $R1 = 0.0318$, $wR2 = 0.0755$ on all data, goodness-of-fit $S = 1.089$; largest difference peak and hole: 1831 and −705 e nm^{-3}.
[13] Crystal structure of [Pr(C_9H_7)$_3$(S)-(−)-MTSO] (**2b**): $C_{35}H_{31}OPrS$, $M_r = 640.60$, monoclinic, $P2_1$, $a = 830.0(2)$, $b = 953.6(3)$, $c = 1749.6(11)$ pm, $\beta = 91.45(4)^\circ$, $V = 1.3843(6)$ nm^3, $Z = 2$, $\rho_{calcd} = 1.537$ g cm^{-3}, $\mu = 1.862$ mm^{-1}, $F(000) = 648$; total no. of reflections 4519, unique reflections 3707 ($R_{int} = 0.0316$). Data/restraints/parameters: 3706/1/345, Flack parameter: −0.03(2). Final R indices: $R1 = 0.0328$, $wR2 = 0.0779$ on data with $I \geq 4\sigma(I)$ and $R1 = 0.0371$, $wR2 = 0.0805$ on all data, goodness-of-fit $S = 1.091$; largest difference peak and hole: 1843 and −1541 e nm^{-3}.
[14] Crystal structure of [Nd(C_9H_7)$_3$ · DPSO] (**7**): $C_{39}H_{31}NdOS$, $M_r = 691.98$, triclinic, $P\bar{1}$, $a = 953.5(2)$, $b = 1293.4(4)$, $c = 1296.6(7)$ pm, $\alpha = 88.55(4)$, $\beta = 83.10(3)$, $\gamma = 76.56(2)^\circ$, $V = 1.544(1)$ nm^3, $Z = 2$, $\rho_{calcd} = 1.488$ g cm^{-3}, $\mu = 1.779$ mm^{-1}, $F(000) = 698$; reflections (total number) : 9542, unique reflections 7136 ($R_{int} = 0.0249$). Data/restraints/parameters: 7105/0/379. Final R indices: $R1 = 0.0452$, $wR2 = 0.1087$ on data with $I \geq 4\sigma(I)$ and $R1 = 0.0561$, $wR2 = 0.1257$ on all data, goodness-of-fit $S = 1.066$; largest difference peak and hole: 1983 and −1707 e nm^{-3}.
[15] Crystal structure of [La(C_5H_5)$_3$(R)-(+)-MTSO] (**8a**): $C_{23}H_{25}LaOS$, $M_r = 488.42$, orthorhombic, $P2_12_12_1$, $a = 879.4(1)$, $b = 1192.0(4)$, $c = 2103(2)$ pm, $V = 2.204(2)$ nm^3, $Z = 4$, $\rho_{calcd} = 1.472$ g cm^{-3}, $\mu = 2.041$ mm^{-1}, $F(000) = 976$; total no. of reflections 4785, unique 3997 ($R_{int} = 0.0293$). Data/restraints/parameters: 3996/0/246, Flack parameter: 0.02(4). Final R indices: $R1 = 0.0462$, $wR2 = 0.1096$ on data with $I \geq 4\sigma(I)$ and $R1 = 0.0518$, $wR2 = 0.1157$ on all data; goodness-of-fit $S = 1.165$, largest difference peak and hole: 1152 and −2098 e nm^{-3}.
[16] Crystal structure of [Pr(C_5H_5)$_3$(R)-(+)-MTSO] (**9a**): $C_{23}H_{25}OPrS$, $M_r = 490.42$, orthorhombic, $P2_12_12_1$, $a = 873.4(2)$, $b = 1183.9(2)$, $c = 2092.7(6)$ pm, $V = 2.1639(7)$ nm^3, $Z = 4$, $\rho_{calcd} = 1.505$ g cm^{-3}, $\mu = 2.356$ mm^{-1}, $F(000) = 984$; total no. of reflections 4732, unique 3946 ($R_{int} = 0.026$). Data/restraints/parameters: 3945/0/255, Flack parameter: −0.05(3). Final R indices: $R1 = 0.0356$, $wR2 = 0.0786$ on data with $I \geq 4\sigma(I)$ and $R1 = 0.0458$, $wR2 = 0.0843$ on all data; goodness-of-fit $S = 1.119$, largest difference peak and hole: 755 and −733 e nm^{-3}.
[17] Crystal structure of [Nd(C_5H_5)$_3$(R)-(+)-MTSO] (**10a**): $C_{23}H_{25}NdOS$, $M_r = 493.76$, orthorhombic, $P2_12_12_1$, $a = 871.0(1)$, $b = 1181.9(4)$, $c = 2086.4(12)$ pm, $V = 2.148$ nm^3, $Z = 4$, $\rho_{calcd} = 1.527$ g cm^{-3}, $\mu = 2.522$ mm^{-1}, $F(000) = 988$; total no. of reflections 4369, unique 4044 ($R_{int} = 0.0314$). Data/restraints/parameters: 4040/0/246, Flack parameter: −0.01(4). Final R indices: $R1 = 0.0468$, $wR2 = 0.1126$ on data with $I \geq 4\sigma(I)$ and $R1 = 0.0520$, $wR2 = 0.1211$ on all data; goodness-of-fit $S = 1.149$, largest difference peak and hole: 1027 and −2978 e nm^{-3}.
[18] Crystal structure of [La(C_5H_5)$_3$ · DPSO] (**13**): $C_{27}H_{25}LaOS$, $M_r = 536.47$, monoclinic, $P2_1/c$, $a = 1571(3)$, $b = 1798(4)$, $c = 843.2(7)$ pm, $\beta = 92.86(10)^\circ$, $V = 2.378(7)$ nm^3, $Z = 4$, $\rho_{calcd} = 1.498$ g cm^{-3}, $\mu = 1.899$ mm^{-1}, $F(000) = 1072$; total no. of reflections 8180, unique 5478 ($R_{int} = 0.0368$). Data/restraints/parameters: 5474/0/318. Final R indices: $R1 = 0.0291$, $wR2 = 0.0616$ on data with $I \geq 4\sigma(I)$ and $R1 = 0.0443$, $wR2 = 0.0691$ on all data; goodness-of-fit $S = 1.028$, largest difference peak and hole: 752 and −538 e nm^{-3}.
[19] Crystal structure of [Pr(C_5H_5)$_3$ · DPSO] (**14**): $C_{27}H_{25}OPrS$, $M_r = 538.47$, monoclinic, $P2_1/c$, $a = 1571(3)$, $b = 1798(4)$, $c = 843.2(7)$ pm, $\beta = 92.86(10)^\circ$, $V = 2.378(7)$ nm^3, $Z = 4$, $\rho_{calcd} = 1.504$ g cm^{-3}, $\mu = 2.152$ mm^{-1}, $F(000) = 1080$; total no. of reflections 8103, unique reflections 5478 ($R_{int} = 0.0326$). Data/restraints/parameters: 5474/5/271. Final R indices: $R1 = 0.0348$, $wR2 = 0.0820$ on data with $I \geq 4\sigma(I)$ and $R1 = 0.0501$, $wR2 = 0.0921$ on all data; goodness-of-fit $S = 1.018$, largest difference peak and hole: 1169 and −788 e nm^{-3}.
[20] J. Petersen, E. Lork, R. Mews, *Chem. Commun.* **1996**, 2593.
[21] U. de la Camp, H. Hope, *Acta Crystallogr. Sect. B* **1970**, *26*, 846.
[22] A. D. Sherry, C. F. G. C. Geraldes, in *Lanthanide Probes in Life, Chemical and Earth Sciences*, (Eds.: J.-C. G. Bünzli, G. R. Choppin), Elsevier, Amsterdam, **1989**, p. 100 (Table 4.1), and references therein.
[23] J. Guan, Ph. D. Thesis, University of Hamburg, **1998**, p. 61.
[24] See: F. A. Cotton, in *Dynamic Nuclear Magnetic Resonance Spectroscopy*, (Eds.: J. L. Jackman, F. A. Cotton), Academic Press, New York, **1975**, chapter 10.
[25] P. Bougeard, M. Mancini, B. G. Sayer, M. J. McGlinchey, *Inorg. Chem.* **1985**, *24*, 93.
[26] For earlier reports on f–f CD studies of organolanthanoid complexes see: a) J. Stehr, R. D. Fischer, *J. Organomet. Chem.* **1993**, *459*, 79–86; b) A. Steudel, J. Stehr, R. D. Fischer, E. Siebel , *J. Organomet. Chem.* **1996**, *510*, 197.
[27] See: a) W. Kuhn, in *Stereochemie*, (Ed.: K. Freudenberg), Deuticke, Leipzig, **1933**, p. 397; b) H. Okawa, S. Kida, S. Misumi, *Bull. Chem. Soc. Jap.* **1984**, *57*, 3147, and references therein.
[28] F. S. Richardson, *Inorg. Chem.* **1980**, *19*, 2806.
[29] H. Okawa, M. Nakamura, Y. Shuin, S. Kida, *Bull. Chem. Soc. Jap.* **1986**, *59*, 3657.
[30] A. Steudel, E. Siebel, R. D. Fischer, G. Paolucci, V. Lucchini, *J. Organomet. Chem.* **1998**, *556*, 229.
[31] A. Steudel, Ph. D. Thesis, University of Hamburg, **1997**, p. 106.
[32] W.-W. Ma, Z.-Z. Wu, R.-F. Cai, Z.-E. Huang, J. Sum, *Polyhedron* **1997**, *16*, 3723.
[33] a) H. B. Kagan, *Stereochemie*, Thieme, Stuttgart, **1979**; b) S. F. Mason, *Molecular Optical Activity and Chiral Discriminations*, Cambridge University Press, Cambridge, **1982**.
[34] a) G. M. Sheldrick, SHELX-86; *Acta Crystallogr.* **1990**, *A46*, 467; b) G. M. Sheldrick, Program for the Refinement of Crystal Structures, Universität Göttingen, Germany, **1993**; c) G. M. Sheldrick, SHELXPLUS, Release 4.21/v, Siemens Analytical X-Ray Instruments, Madison, Wisconsin (USA).

Received: October 8, 1998 [F1385]